

Measuring Interactions in a Bose-Einstein Condensate Using Imbalanced Dynamical Decoupling

Hagai Edri, Boaz Raz, Gavriel Fleurov, Roei Ozeri and Nir Davidson

Department of Physics of Complex Systems, Weizmann Institute of Science, Rehovot 7610001, Israel

We measure inter-state interactions in a Bose-Einstein Condensate (BEC) set in a superposition of two states, using microwave spectroscopy. We introduce a population imbalanced dynamic-decoupling scheme that accumulates a phase due to inter-state interactions while canceling intra-state density shifts and external noise sources. Uncertainties of the measured scattering lengths were $0.02a_0$ (where a_0 is the Bohr radius) for both magnetic sensitive and insensitive transitions, indicating that we successfully decoupled our system from strong magnetic noises. We experimentally show that the Bloch sphere representing general superposition states is "twisted" by the nonlinear interactions, as predicted in [1] and that the twist rate depends on the difference between inter-state and intra-state scattering lengths $a_{22} + a_{11} - 2a_{12}$. Our results allow for a better understanding of inter-atomic potentials in ^{87}Rb . Our scheme can be used for spin squeezing and observing polaron physics close to a Feshbach resonance, where interactions diverge, and strong magnetic noises are ever present.

Interactions play a primary role in ultracold gases, from cooling process to changing a systems ground state and driving quantum phase transitions. In the cold collision regime, interaction strength is parameterized by an s -wave scattering length a_{ij} , where $|i\rangle, |j\rangle$ are two internal states of the interacting atoms (i.e. Zeeman states or hyperfine levels). Our knowledge of these interactions comes from spectroscopic measurements [1, 2], observing collective oscillations [3], position of Feshbach resonances [4–6] and thermalization experiments [7, 8], which are then taken into account for calibrations of detailed calculations of inter-atomic potentials [9, 10]. Precise knowledge of inter-state interaction parameters is important for spin squeezing [11], polaron physics [12–15], BEC solitons [16, 17], spinor and binary BECs [18, 19], and magnons [20].

Frequency shifts in population-balanced microwave Ramsey spectroscopy due to mean-field interactions were used to measure intra-state scattering length differences $a_{22} - a_{11}$ for both thermal ultra cold boson [21] and BEC [1] (and their absence observed for both thermal [22] and quantum degenerate [23] ultracold Fermi gases). In population-imbalanced transitions an additional term in the frequency shift of the transition, proportional to $a_{22} + a_{11} - 2a_{12}$ and to the density difference between the states was predicted but was too small to be measured [1]. These measurements were limited to magnetic insensitive transitions where magnetic noises are largely suppressed. Dynamic decoupling (DD) could decouple the system from these magnetic noises and preserve its coherence over long times by applying a set of spin rotations. It also decouples it from the intra-state interactions and can not be applied to measure them.

Dynamic decoupling was demonstrated in NMR [24, 25], spins in solids [26–28], ultracold atoms [29, 30], and trapped ions [31–33]. DD aims to decouple a system from its environment, to measure a signal along with DD, one can modulate the system itself synchronously with the DD scheme [34–36], in a similar fashion to how a

lock-in amplifier operates. However, this modulation can generate noises that are in phase with the DD scheme, and requires control of the signal you are interested in.

In this letter, we propose and demonstrate a method for measuring interactions in ultracold gases in a noisy environment with a long coherence time and increased sensitivity to inter-state interactions. Our measurements are based on a population imbalanced DD scheme (Fig. 1) that accumulates the effect of inter-state interactions between ultracold atoms in two internal states, without adding any modulation besides the DD itself. We fully characterize the process [37], confirming the prediction of [1] that the Bloch sphere of the two states is twisted by the inter-state interaction and from the measured twist determine $a_{22} + a_{11} - 2a_{12}$ with $0.02 a_0$ sensitivity for both magnetic sensitive and insensitive transitions.

We use a Bose-Einstein condensate (BEC) of ultracold ^{87}Rb atoms in states $|1\rangle = |F=1, m_{f_1}\rangle$ and $|2\rangle = |F=2, m_{f_2}\rangle$, where F is the total spin of the atom and $m_{f_{1,2}}$ is the spin projection on the magnetic field axis. In the mean-field approximation the two states undergo energy shifts,

$$\begin{aligned}\delta E_1 &= \frac{4\pi\hbar^2}{m}(\alpha_{11}a_{11}n_1 + \alpha_{12}a_{12}n_2), \\ \delta E_2 &= \frac{4\pi\hbar^2}{m}(\alpha_{22}a_{22}n_2 + \alpha_{12}a_{12}n_1),\end{aligned}\tag{1}$$

$n_{1,2}$ are the densities in the different states, a_{ij} are the s -wave scattering lengths, α_{ij} are correlation factors that account for Bose statistics (for a thermal cloud $\alpha_{ij} = 2$, and for a BEC $\alpha_{ij} = 1$ [1]), m is the atomic mass, and \hbar is the reduced Planck constant. The energy difference between the two states in a BEC is,

$$\begin{aligned}\delta E_2 - \delta E_1 &= \frac{2\pi\hbar^2}{m} \left((a_{22} - a_{11})(n_2 + n_1) \right. \\ &\quad \left. + (a_{22} + a_{11} - 2a_{12})(n_2 - n_1) \right).\end{aligned}\tag{2}$$

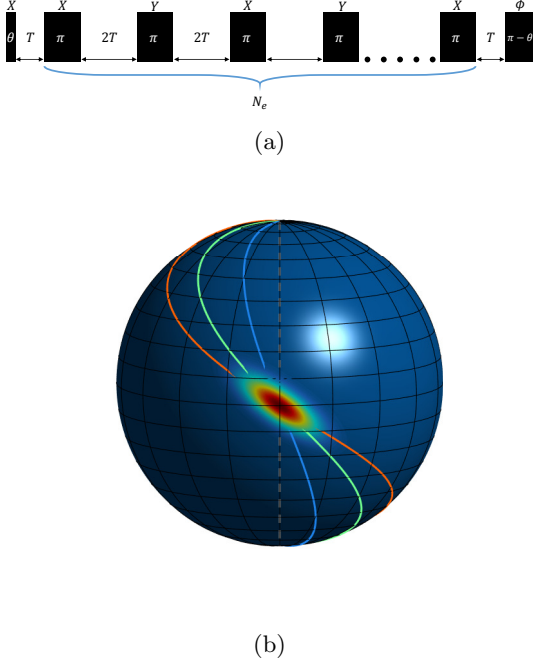


FIG. 1: Imbalanced dynamic decoupling. (a) Pulse sequence. An initial pulse of area θ , followed by a set of N_e echo pulses around X,Y axis, separated by time $2T$, with a final pulse with area $\pi - \theta$ and phase ϕ . The initial pulse creates a superposition $\cos \frac{\theta}{2} |1\rangle + \sin \frac{\theta}{2} |2\rangle$, with density difference $\delta n = n(\sin^2 \frac{\theta}{2} - \cos^2 \frac{\theta}{2})$, where n is the total density. (b) A twisted Bloch sphere after imbalanced DD. The evolution of states at different latitudes as we increase the DD time is shown by longitudes (dashed grey to blue ,green and red). A coherent state around the equator gets squeezed and twisted, shown by the colored distribution.

The first term is proportional to the sum of densities $n = n_1 + n_2$, while the second one is proportional to the density difference $\delta n = n_2 - n_1$. A typical Ramsey experiment starts with the atoms in state $|1\rangle$, a first $\pi/2$ pulse transfers the atoms to the state $\frac{1}{\sqrt{2}}(|1\rangle + |2\rangle)$, and after a holding time T a second $\pi/2$ pulse converts the phase shift between the states to population difference. During the interrogation time, the population in the two states is equal, which makes the second term in eq. (2) vanish and the phase between the two states depends only on the sum of densities. However, we can start with a finite density difference by applying a pulse with area $\theta \neq \pi/2$ which transfers the atoms to the state $\cos \frac{\theta}{2} |1\rangle + \sin \frac{\theta}{2} |2\rangle$, here the density difference is $\delta n = n(\sin^2 \frac{\theta}{2} - \cos^2 \frac{\theta}{2}) = -n \cos \theta$. Following a Ramsey wait time T we apply a second pulse with area $\pi - \theta$ to convert the phase difference between the two states to population $P = N_2/(N_1 + N_2)$, where $N_{1,2}$ is the corresponding number of atoms in each state.

In our imbalanced DD scheme (Fig. 1 (a)) we apply a number of echo pulses (N_e) between two pulses

of θ and $\pi - \theta$, with alternating phase of $0^\circ, 90^\circ$ to rotate the state around X,Y axis in the Bloch sphere, this scheme adds several benefits. First, it cancels the first term in eq. (2), because the sum of densities does not change following a π pulse, it also nullifies any inhomogeneous dephasing mechanisms (e.g. due to inhomogeneous density) and spatial phase evolution [38], which allows a longer coherence time. Second, other quasi-static external noises are cancelled as well (magnetic fields, light shifts etc.). The echo pulses reverse the sign of the density difference δn in a similar fashion to how a lock-in amplifier operates. Therefore, we accumulate phase due to the second term in eq. 2 and achieve an increased sensitivity to $a_{22} + a_{11} - 2a_{12}$, which is typically much smaller than $a_{22} - a_{11}$. Rotating the Bloch vector around X,Y cancels noises in the control pulses [27, 39, 40] and also renders the rotations symmetric with respect to the equator in the Bloch sphere in any XYXY block. Thus, any phase accumulated due to population imbalance during the pulses is equal in the upper and lower halves of the Bloch sphere.

The calculated population in state $|2\rangle$ at the end of this sequence, is given by (for detailed calculation see [41]),

$$P = \frac{1}{4} \left[2 \sin^2 \theta \cos \left(\phi - \frac{gn}{\hbar} N_e T \cos \theta \right) + \cos 2\theta + 3 \right] \quad (3)$$

where ϕ is the phase of the last pulse and $g = \frac{4\pi\hbar^2}{m} (a_{11} + a_{22} - 2a_{12})$ is the interaction shift. This interaction twists the Bloch sphere (Figure 1(b)), where the upper hemisphere rotates in one direction and the lower hemisphere rotates in the opposite direction.

This method can be used for spin squeezing, similar to [11], owing to the long coherence time in our scheme it is possible to generate a spin squeezed state even with weak interactions. It is also relevant for polaron physics, where a minority of atoms in state $|1\rangle$ interact strongly with a majority of atoms in state $|2\rangle$. The strong interaction dresses the minority atoms into quasi-particles, known as polarons. The lifetime and energy of polarons have been observed recently [14, 15, 42–44]. Imbalanced DD can be used to increase coherence in these measurements, which will, in turn, increase spectroscopic resolution.

In our system we trap a BEC of $\sim 5 \times 10^5$ ^{87}Rb atoms in a crossed dipole trap with trapping frequencies of $(\omega_x, \omega_y, \omega_z) = 2\pi \times (31, 37, 109)$ Hz. We use MW radiation close to 6.834 GHz to drive transitions between different hyperfine levels in a magnetic field of 2.067 G. We drive both the magnetic insensitive transition $|1,0\rangle \leftrightarrow |2,0\rangle$ and magnetic sensitive transitions $|1,1\rangle \leftrightarrow |2,0\rangle$, $|1,1\rangle \leftrightarrow |2,2\rangle$, which are separated by a large Zeeman splitting $\Delta \gg \Omega_R$, here Ω_R is the Rabi frequency of our MW radiation.

To perform an imbalanced DD scheme, we start with all atoms in the state $|1\rangle = |1,0\rangle$ (magnetic insensitive transition) or $|1\rangle = |1,1\rangle$ (magnetic sensitive transitions) and apply MW pulses to couple to state $|2\rangle = |2,0\rangle$ or $|2\rangle = |2,2\rangle$. We apply a pulse of length t_p to rotate

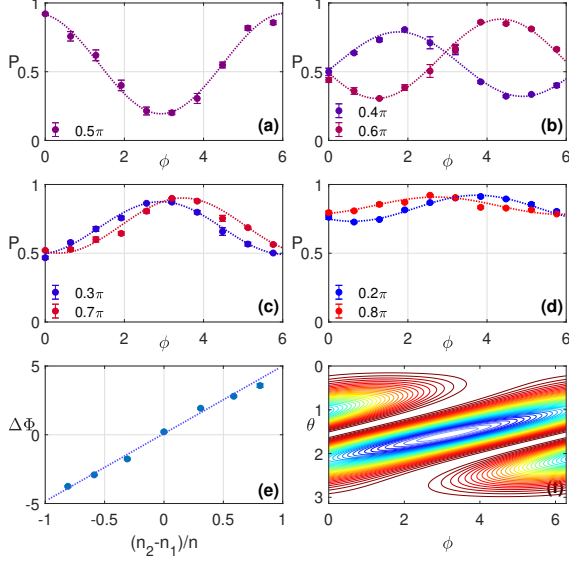


FIG. 2: Measurements for $|1,0\rangle \leftrightarrow |2,0\rangle$ transition after 16 echo pulses with arm time $T = 3$ ms, giving a total time of 96ms. (a-d) Measured population P while scanning the phase of the last pulse for different θ (initial density difference $\propto \cos\theta$), showing clear fringes (dotted lines are fits to the data). The fringes are phase shifted, due to interactions and density difference δn (e) Phase shift as a function of population imbalance. The phase shift is proportional to the density difference δn (Points are phase shifts found by the fits in (a-d), dotted line is a linear fit). (f) A 2D fit to all of the data in (a-d) (following eq. 3) showing a twisted Bloch sphere.

the Bloch vector around the X axis with a polar angle $\theta = \Omega_R t_p$. We let the state evolve for a time T and apply a π pulse to invert the populations. We then alternate between π pulses around the X and the Y axis with free evolution time of $2T$ in between (similar to a XY8 sequence [45]). Finally, after another hold time T we apply a pulse $\pi - \theta$ with phase ϕ to rotate the vector around the axis $\cos\phi X + \sin\phi Y$. An illustration of our pulse sequence is shown in Fig. 1 (a). The train of echo pulses can be prolonged to accumulate more phase and increase sensitivity to g . We used up to 72 echo pulses.

At the end of the sequence we released the cloud from the trap and let it expand for 20 ms. We measured the population in state $|2\rangle$ using a normalized detection scheme. We measured the Thomas-Fermi radius of the cloud in order to calculate the chemical potential and average density of the BEC.

Our measurements on the magnetic insensitive transition ($|1,0\rangle \leftrightarrow |2,0\rangle$) after 16 echo pulses with arm time $T = 3$ ms (total time of 96 ms) are shown in Fig.2 (a-d), filled circles are the measured P vs ϕ (errorbars indicate one standard deviation of the mean of four measurements), where different colors indicate different θ . The

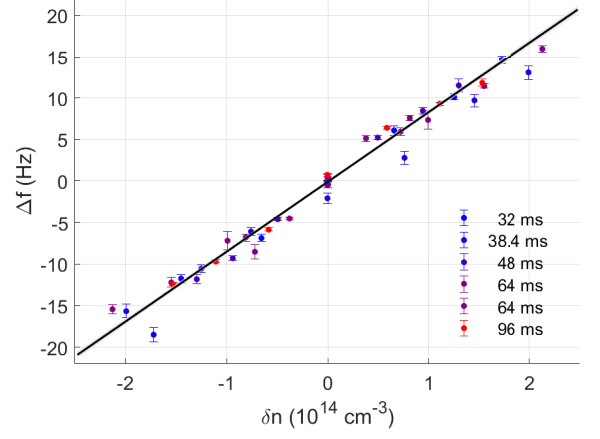


FIG. 3: Frequency shift due to interactions between $|2,0\rangle \leftrightarrow |1,0\rangle$ - Measured frequency shift $\Delta f = \frac{\Delta\Phi}{2\pi T_{\text{tot}}}$ and density difference δn from measurements of imbalanced DD with different number of echo pulses and arm times. A linear fit to the data (black line, one standard deviation in gray) gives a scattering length difference of $(a_{11} + a_{22} - 2a_{12})_{1,0 \rightarrow 2,0} = 1.10 \pm 0.02 a_0$, showing the high precision that can be achieved in this method.

dotted lines are fits to $C \cos(\phi + \Delta\phi) + B$, where C is the contrast, ϕ is the phase of the last pulse, $\Delta\phi$ is the phase shift, and B is the bias. The contrast of the fringe with $\theta = \frac{\pi}{2}$ (Fig. 2 (a)) is high, showing high coherence after a long DD time of 96 ms, compared with our typical Ramsey coherence time of ~ 15 ms [46]. When we change θ the contrast decreases, as expected from Eq.3, but there are clear fringes in all cases (Fig. 2 (b-d)) and excellent agreement with our fit. A phase shift is present in all measurements, and it is linear with respect to δn (Fig. 2 (e)) as predicted by Eq. (3). We also fit all the data to Eq. (3) showing a twisted Bloch sphere (Fig. 2 (f)).

To validate our measurement and test the performance of this sequence. We repeated this measurement for different times $T_{\text{tot}} = 2N_e T$ with different arm times T and number of echoes N_e . Our measurement time was limited by inelastic collisions of atoms in state $|2,0\rangle$, transferring them to states $|2,-1\rangle$ and $|2,1\rangle$ [47]. The frequency shift we measured $\Delta f = \frac{\Delta\Phi}{2\pi T_{\text{tot}}}$ grows linearly with the density difference δn (Fig. 3). From a linear fit we get $(a_{11} + a_{22} - 2a_{12})_{1,0 \rightarrow 2,0} = 1.10 \pm 0.02 a_0$ (statistical error of one standard deviation), showing the high accuracy and signal to noise ratio achieved with imbalanced DD. Our main source of systematic errors is the measurement of density of the BEC, we estimate it to be 16%. This measurement of scattering length difference can be used to calculate interatomic potentials. Using a known value for $a_{11} = 94.69 a_0$ [9] and previously measured $a_{22} - a_{11} = -1.40 \pm 0.04 a_0$ in our setup [46], we can estimate $a_{12} = 93.44 \pm 0.02 a_0$ and

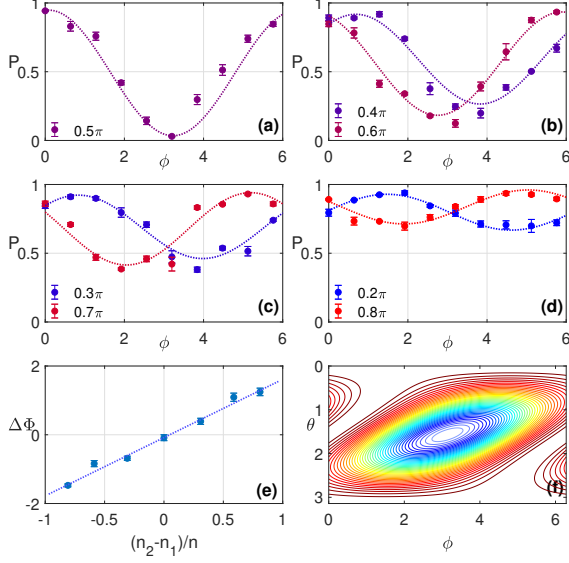


FIG. 4: Measurements for magnetic sensitive transition $|1, 1\rangle \leftrightarrow |2, 0\rangle$ after 56 echo pulses with arm time $T = 0.42$ ms, giving a total time of 47ms. The short arm time T is needed for keeping high coherence in the presence of strong magnetic noises. (a-d) Measured population P while scanning the phase of the last pulse for different θ (initial density difference $\propto \cos\theta$), showing clear fringes (dotted lines are fits to the data). The fringes are phase shifted, due to interactions and density difference δn (e) Phase shift as a function of population imbalance. The phase shift is proportional to the density difference δn (Points are phase shifts found by the fits in (a-d), dotted line is a linear fit). (f) A 2D fit to all of the data in (a-d) (following eq. 3) showing a twisted Bloch sphere.

$\frac{a_{11} + a_{22} - 2a_{21}}{a_{22} - a_{11}} = -0.78 \pm 0.03$. This ratio is insensitive to systematic errors in estimating density.

We perform the same measurement as before on two magnetic sensitive transitions, $|1, 1\rangle \leftrightarrow |2, 0\rangle$ and $|1, 1\rangle \leftrightarrow |2, 2\rangle$ with a magnetic field sensitivity of 0.7 kHz/mG and 2.1 kHz/mG respectively. Our main magnetic noise source is the 50 Hz AC from the electricity grid of ~ 1 mG peak to peak at the position of the atoms. Our results for $|1, 1\rangle \leftrightarrow |2, 0\rangle$ transition for 56 echo pulses and an arm time of $T = 0.42$ ms (Fig. 4), are similar to our results for the magnetic insensitive transition. We get long coherence times and a phase shift that is proportional to the density difference δn . Our Ramsey coherence time for magnetic sensitive transition is a few milliseconds due to magnetic noises, with DD we are able to increase it, and measure fringes with high coherence after a total time of 47ms.

We repeated this measurement for different times T_{tot} with different arm times T and number of echoes N_e for the two magnetic sensitive transitions, and measured

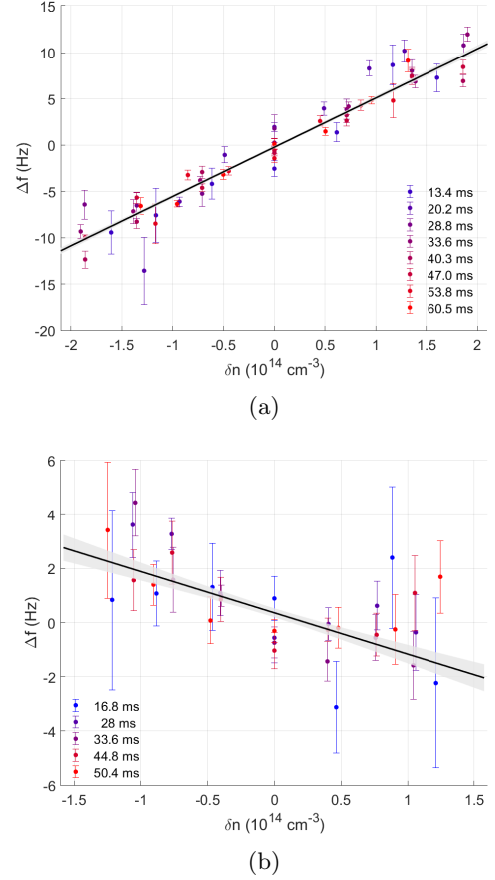


FIG. 5: Frequency shift due to interactions in magnetic transitions - The measured frequency shift Δf and density difference δn from repeated measurements of imbalanced DD with different number of echo pulses and arm times for $|1, 1\rangle \leftrightarrow |2, 0\rangle$ (a) and $|1, 1\rangle \leftrightarrow |2, 2\rangle$ (b). A linear fit to the data (black line, one standard deviation in gray) gives a scattering length difference of (a) $(a_{11} + a_{22} - 2a_{12})_{1,1 \rightarrow 2,0} = 0.69 \pm 0.02a_0$ and (b) $(a_{11} + a_{22} - 2a_{12})_{1,1 \rightarrow 2,2} = -0.20 \pm 0.04a_0$ showing high signal to noise ratio that can be achieved in this method even in the presence of strong magnetic noise.

a frequency shift Δf that grows linearly with the density difference (Fig. 5). From a linear fit we estimate $(a_{11} + a_{22} - 2a_{21}) = 0.69 \pm 0.02a_0$ for $|1, 1\rangle$ to $|2, 0\rangle$ (Fig. 5 (a)) transition and $(a_{11} + a_{22} - 2a_{21}) = -0.20 \pm 0.04a_0$ for $|1, 1\rangle$ to $|2, 2\rangle$ transition (Fig. 5 (b)), demonstrating good accuracy and signal to noise ratio even in a noisy environment. These measurements can be performed close to a Feshbach resonance where typically there are no magnetic insensitive transitions and one of the scattering lengths a_{11}, a_{22} or a_{12} diverges. This increase in interaction will result in larger phase shifts and can be used to generate spin squeezed states [11].

We introduced and demonstrated a novel and sensitive method, based on imbalanced dynamical decoupling, for

measuring interactions in ultracold atoms from the twist of the Bloch sphere caused by the interactions. Our precision is comparable to other measurement done on a magnetic insensitive transition $|1, -1\rangle \leftrightarrow |2, 1\rangle$ [1, 3], and we show similar precision with magnetic sensitive transitions. The scattering length difference we measure for three transitions in ^{87}Rb can be used to calculate interatomic potentials. The interactions between imbalanced populations generate a phase shift that is accumulated in our sequence without having to externally perturb the system, as in other DD schemes [34, 35]. This type of

interactions are of great interest in polaron physics [12–15], spin squeezing [48], and solitons [49]. This method can be used to increase sensitivity in ultracold atoms experiments studying these phenomena.

ACKNOWLEDGMENTS

The authors would like to thank Yotam Shapira and Tom Manovitz for fruitful discussions.

-
- [1] D. Harber, H. Lewandowski, J. McGuirk, and E. A. Cornell, *Physical Review A* **66**, 053616 (2002).
 - [2] C. Fertig and K. Gibble, *Physical review letters* **85**, 1622 (2000).
 - [3] M. Egorov, B. Opanchuk, P. Drummond, B. Hall, P. Hannaford, and A. Sidorov, *Physical Review A* **87**, 053614 (2013).
 - [4] S. Knoop, T. Schuster, R. Scelle, A. Trautmann, J. Appmeier, M. K. Oberthaler, E. Tiesinga, and E. Tiemann, *Phys. Rev. A* **83**, 042704 (2011).
 - [5] F. Ferlaino, C. D’Errico, G. Roati, M. Zaccanti, M. Inguscio, G. Modugno, and A. Simoni, *Phys. Rev. A* **73**, 040702 (2006).
 - [6] A. J. Kerman, C. Chin, V. Vuletić, S. Chu, P. J. Leo, C. J. Williams, and P. S. Julienne, *Comptes Rendus de l’Académie des Sciences-Series IV-Physics* **2**, 633 (2001).
 - [7] C. Marzok, B. Deh, P. W. Courteille, and C. Zimmermann, *Phys. Rev. A* **76**, 052704 (2007).
 - [8] G. Ferrari, M. Inguscio, W. Jastrzebski, G. Modugno, G. Roati, and A. Simoni, *Phys. Rev. Lett.* **89**, 053202 (2002).
 - [9] E. Van Kempen, S. Kokkelmans, D. Heinzen, and B. Verhaar, *Physical review letters* **88**, 093201 (2002).
 - [10] B. Verhaar, E. Van Kempen, and S. Kokkelmans, *Physical Review A* **79**, 032711 (2009).
 - [11] C. Gross, T. Zibold, E. Nicklas, J. Esteve, and M. K. Oberthaler, *Nature* **464**, 1165 (2010).
 - [12] C. Kohstall, M. Zaccanti, M. Jag, A. Trenkwalder, P. Massignan, G. M. Bruun, F. Schreck, and R. Grimm, *Nature* **485**, 615 (2012).
 - [13] A. Schirotzek, C.-H. Wu, A. Sommer, and M. W. Zwierlein, *Phys. Rev. Lett.* **102**, 230402 (2009).
 - [14] M.-G. Hu, M. J. Van de Graaff, D. Kedar, J. P. Corson, E. A. Cornell, and D. S. Jin, *Physical review letters* **117**, 055301 (2016).
 - [15] N. B. Jørgensen, L. Wacker, K. T. Skalmstang, M. M. Parish, J. Levinsen, R. S. Christensen, G. M. Bruun, and J. J. Arlt, *Physical review letters* **117**, 055302 (2016).
 - [16] C. Hamner, Y. Zhang, J. J. Chang, C. Zhang, and P. Engels, *Phys. Rev. Lett.* **111**, 264101 (2013).
 - [17] T. M. Bersano, V. Gokhroo, M. A. Khomehchi, J. D’Ambrose, D. J. Frantzeskakis, P. Engels, and P. G. Kevrekidis, *Phys. Rev. Lett.* **120**, 063202 (2018).
 - [18] D. M. Stamper-Kurn and M. Ueda, *Rev. Mod. Phys.* **85**, 1191 (2013).
 - [19] K. M. Mertes, J. W. Merrill, R. Carretero-González, D. J. Frantzeskakis, P. G. Kevrekidis, and D. S. Hall, *Phys. Rev. Lett.* **99**, 190402 (2007).
 - [20] G. E. Marti, A. MacRae, R. Olf, S. Lourette, F. Fang, and D. M. Stamper-Kurn, *Phys. Rev. Lett.* **113**, 155302 (2014).
 - [21] K. Gibble and S. Chu, *Phys. Rev. Lett.* **70**, 1771 (1993).
 - [22] M. W. Zwierlein, Z. Hadzibabic, S. Gupta, and W. Ketterle, *Phys. Rev. Lett.* **91**, 250404 (2003).
 - [23] S. Gupta, Z. Hadzibabic, M. Zwierlein, C. Stan, K. Dieckmann, C. Schunck, E. Van Kempen, B. Verhaar, and W. Ketterle, *Science* **300**, 1723 (2003).
 - [24] D. Haar, *Fluctuation, Relaxation and Resonance in Magnetic Systems: Scottish Universities’ Summer School 1961* (Oliver & Boyd, 1962).
 - [25] U. Haeberlen, *High Resolution NMR in Solids: Advances in Magnetic Resonance* (Academic Press, 1976).
 - [26] J. Du, X. Rong, N. Zhao, Y. Wang, J. Yang, and R. Liu, *Nature* **461**, 1265 (2009).
 - [27] G. De Lange, Z. Wang, D. Riste, V. Dobrovitski, and R. Hanson, *Science* **330**, 60 (2010).
 - [28] N. Bar-Gill, L. M. Pham, A. Jarmola, D. Budker, and R. L. Walsworth, *Nature communications* **4**, 1743 (2013).
 - [29] Y. Sagi, I. Almog, and N. Davidson, *Physical review letters* **105**, 053201 (2010).
 - [30] I. Almog, Y. Sagi, G. Gordon, G. Bensky, G. Kurizki, and N. Davidson, *Journal of Physics B: Atomic, Molecular and Optical Physics* **44**, 154006 (2011).
 - [31] S. Kotler, N. Akerman, Y. Glickman, and R. Ozeri, *Physical review letters* **110**, 110503 (2013).
 - [32] R. Shaniv, N. Akerman, and R. Ozeri, *Physical review letters* **116**, 140801 (2016).
 - [33] M. J. Biercuk, H. Uys, A. P. VanDevender, N. Shiga, W. M. Itano, and J. J. Bollinger, *Nature* **458**, 996 (2009).
 - [34] S. Kotler, N. Akerman, Y. Glickman, A. Keselman, and R. Ozeri, *Nature* **473**, 61 (2011).
 - [35] R. Shaniv and R. Ozeri, *Nature communications* **8**, 14157 (2017).
 - [36] G. de Lange, D. Ristè, V. V. Dobrovitski, and R. Hanson, *Phys. Rev. Lett.* **106**, 080802 (2011).
 - [37] Y. Sagi, I. Almog, and N. Davidson, *Phys. Rev. Lett.* **105**, 053201 (2010).
 - [38] R. P. Anderson, C. Ticknor, A. I. Sidorov, and B. V. Hall, *Phys. Rev. A* **80**, 023603 (2009).
 - [39] T. Gullion, D. B. Baker, and M. S. Conradi, *Journal of Magnetic Resonance* (1969) **89**, 479 (1990).
 - [40] Z.-H. Wang, G. De Lange, D. Ristè, R. Hanson, and V. Dobrovitski, *Physical Review B* **85**, 155204 (2012).
 - [41] See supplemental material.

- [42] A. Schirotzek, C.-H. Wu, A. Sommer, and M. W. Zwierlein, Physical review letters **102**, 230402 (2009).
- [43] C. Kohstall, M. Zaccanti, M. Jag, A. Trenkwalder, P. Massignan, G. M. Bruun, F. Schreck, and R. Grimm, Nature **485**, 615 (2012).
- [44] G. Ness, C. Shkedrov, Y. Florshaim, and Y. Sagi, arXiv preprint arXiv:2001.10450 (2020).
- [45] M. A. A. Ahmed, G. A. Álvarez, and D. Suter, Physical Review A **87**, 042309 (2013).
- [46] H. Edri, B. Raz, N. Matzliah, N. Davidson, and R. Ozeri, arXiv preprint arXiv:1910.01341 (2019).
- [47] A. Widera, F. Gerbier, S. Fölling, T. Gericke, O. Mandel, and I. Bloch, New Journal of Physics **8**, 152 (2006).
- [48] W. Müssel, H. Strobel, D. Linnemann, D. Hume, and M. Oberthaler, Physical review letters **113**, 103004 (2014).
- [49] B. Eiermann, T. Anker, M. Albiez, M. Taglieber, P. Treutlein, K.-P. Marzlin, and M. Oberthaler, Physical review letters **92**, 230401 (2004).

Supplementary Material for Measuring Interactions in a Bose-Einstein Condensate Using Imbalanced Dynamical Decoupling

Hagai Edri, Boaz Raz, Gavriel Fleurov, Roei Ozeri and Nir Davidson

Department of Physics of Complex Systems, Weizmann Institute of Science,
Rehovot 76100, Israel

Experimental Setup

In our setup we trap ^{87}Rb in a crossed dipole trap ($\lambda = 1064 \text{ nm}$). We produce an almost pure BEC of $\sim 10^5$ atoms with no visible thermal fraction. The trapping frequencies are $\omega_{x,y,z} = 2\pi \times (29, 35, 104)$.

In each measurement we take two images with imaging light that is resonant with the $F = 2 \rightarrow F' = 3$ transition of the ^{87}Rb D2 line after 20 ms time of flight. In the first image we count only the atoms in the state $F = 2$. Then, after a short repump pulse ($F = 1 \rightarrow F' = 2$, $40 \mu\text{s}$) that transfers all atoms from $F = 1$ to the $F = 2$ manifold, we image the cloud again to count the total number of atoms and measure the density. In this way we measure the relative population of state $|2\rangle$, without being susceptible to fluctuations in atom numbers between different measurements.

We measure the number density by fitting the integrated column density in the second image with $f(x) = \text{Max}\left(0, \left(1 - \frac{x^2}{x_c^2}\right)^2\right)$, where x_c is the cloud's

half width in the strong trapping direction. From which we calculate the chemical potential μ and the peak number density $n_0 = \mu \frac{m}{4\pi\hbar^2 a}$, where m is the atomic mass, a is the scattering length, and \hbar is the reduced Planck constant. The average number density is given by $n = \frac{4}{7}n_0$.

Dynamical Decoupling

We use microwave (MW) radiation close to $f_0 = 6.834$ GHz to induce transitions between hyperfine levels of ^{87}Rb atoms, $|1\rangle = |F=1, m_{f_1}\rangle$ and $|2\rangle = |F=2, m_{f_2}\rangle$, where F is the total spin and $m_{f_{1,2}}$ is its projection on the magnetic field axis. We start with all atoms in state $|1\rangle$ and apply a set of pulses to control their state and accumulate phase due to inter-state interactions. Each pulse of length t_p and Rabi frequency Ω_R rotates the state vector by an angle $\theta = \Omega_R t_p$ around the axis $\hat{n} = \cos\phi\hat{x} + \sin\phi\hat{y}$. This rotation can be applied to any state $|\psi\rangle = \alpha|1\rangle + \beta|2\rangle$ with arbitrary α and β by an operator $R_{\hat{n}}(\theta) = \exp(\frac{i}{2}\theta\vec{\sigma} \cdot \hat{n})$. Free evolution of the state for a time T corresponds to a rotation around the \hat{z} axis on the Bloch sphere. The angle of rotation is $\epsilon = \frac{\delta E_{12}}{\hbar}T$, where δE_{12} is the energy difference between the two levels (Eq. (2) in the main text).

Our pulse sequence starts with a pulse of θ around the \hat{x} axis followed by a train of π pulses around X-Y-X-Y-Y-X-Y-X axes with a free evolution time $2T$ between pulses (XY8 sequence), we then apply a pulse of $\pi - \theta$ around

an axis \hat{n} . Applying all these rotations amounts to:

$$M(\theta, \phi) = R_{\hat{n}}(\pi - \theta) R_{\hat{z}}(\epsilon) R_{\hat{x}}(\pi) R_{\hat{z}}(2\tilde{\epsilon}) R_{\hat{y}}(\pi) R_{\hat{z}}(2\epsilon) R_{\hat{x}}(\pi) R_{\hat{z}}(2\tilde{\epsilon}) R_{\hat{y}}(\pi) R_{\hat{z}}(2\epsilon) \\ R_{\hat{y}}(\pi) R_{\hat{z}}(2\tilde{\epsilon}) R_{\hat{x}}(\pi) R_{\hat{z}}(2\epsilon) R_{\hat{y}}(\pi) R_{\hat{z}}(2\tilde{\epsilon}) R_{\hat{x}}(\pi) R_{\hat{z}}(\epsilon) R_{\hat{x}}(\theta), \quad (1)$$

where $\tilde{\epsilon}$ has inverted populations compared to ϵ , such that $\tilde{\epsilon} - \epsilon$ is proportional to the difference in densities between states $|1\rangle$ and $|2\rangle$, and does not depend on the sum of densities. We calculate the population in state $|2\rangle$ after applying this sequence starting from state $|1\rangle$,

$$P = |M(\theta, \phi) |1\rangle|^2 = \frac{1}{4} \left[2 \sin^2 \theta \cos \left(\phi - \frac{gn}{\hbar} N_e T \cos \theta \right) + \cos 2\theta + 3 \right] \quad (2)$$

where ϕ is the phase of the last pulse, $g = \frac{4\pi\hbar^2}{m} (a_{11} + a_{22} - 2a_{12})$ is the interaction shift and n is the sum of densities in states $|1\rangle$ and $|2\rangle$. In this sequence, the accumulated phase depends solely on the difference in densities $\delta n = -n \cos \theta$.

An advantage of a dynamic decoupling (DD) scheme is it cancels external noises that are slower than our pulse rate $1/T$, which allows us to measure small frequency shifts in a noisy environment for magnetic sensitive transitions. Our main source of magnetic noise is the 50 Hz signal of the electricity grid in our lab. We measured it using short Ramsey spectroscopy (0.15 ms Ramsey time) on the magnetic sensitive transition $|1, 1\rangle \leftrightarrow |2, 2\rangle$, with our $\frac{\pi}{2}$ MW pulses synchronised to the 50 Hz signal. We changed the delay time between the pulses and the 50 Hz signal and scanned the phase of the second MW pulse. The results are shown in Fig. 1, each column is a Ramsey phase scan fringe. It is clear that the phase of the fringes changes as we change the

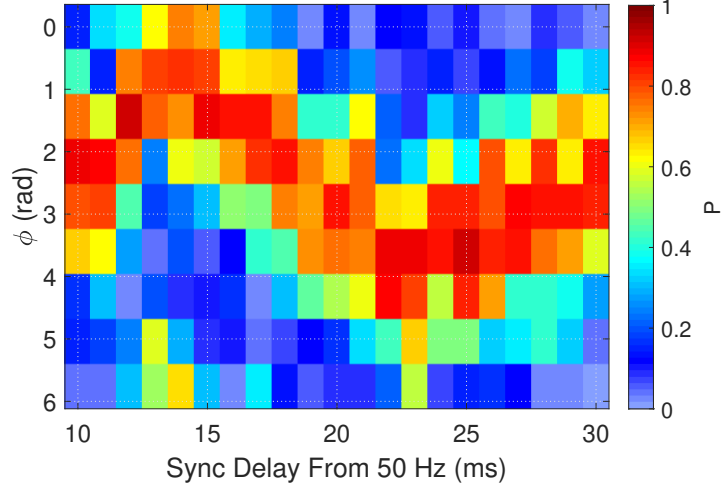


Figure 1: 50 Hz Noise - Ramsey phase scan with Ramsey time of 0.15 ms, with magnetic sensitive transition $|1, 1\rangle \rightarrow |2, 2\rangle$. We changed the delay time between our Ramsey pulses and 50 Hz signal from the electricity grid in our lab. We measured a phase shift that is proportional to the magnetic field noise at 50 Hz as seen by the atoms. The magnetic field at 50 Hz has a 1.31 ± 0.12 mG peak to peak amplitude.

delay time from the 50 Hz signal (horizontal axis). The 50 Hz noise is clearly seen in our measurement, and it has 1.31 ± 0.12 mG peak to peak amplitude, we do not see any other significant noise frequencies. To cancel this noise we use DD with short arm time T of 0.35 – 0.42 ms when measuring on the magnetic sensitive transition.

Inelastic Collisions

The DD scheme increases our coherence time from ~ 15 ms to ~ 100 ms (for magnetic insensitive transition) and from ~ 1 ms to ~ 50 ms (for magnetic sensitive transitions). Our main limitation for the magnetic insensitive

transition are inelastic collisions of atoms in state $|2, 0\rangle$, transferring them to states $|2, -1\rangle$ and $|2, 1\rangle$. We can measure the rate of these collisions by holding all atoms in state $|2, 0\rangle$ for different times and measuring the population of different spin states in $F = 2$. We do that with a Stern-Gerlach measurement, we release the atoms from the trap and turn on a magnetic field with a constant gradient, after 20 ms time of flight the states are well separated in our images. The result of these measurements are presented in fig. 2. The population in $|2, 0\rangle$ decays, while the population of $|2, -1\rangle$ and $|2, 1\rangle$ increases almost by the same amount. From an exponential fit we estimate the spin relaxation time to be 105 ± 2 ms. It does not have an effect on the phase shift in our measurement, and only causes a slightly decreased coherence of our fringes, as can be seen in Fig. 2(a) in the main text, where there is a constant bias due to the population of states $|2, -1\rangle$ and $|2, 1\rangle$.

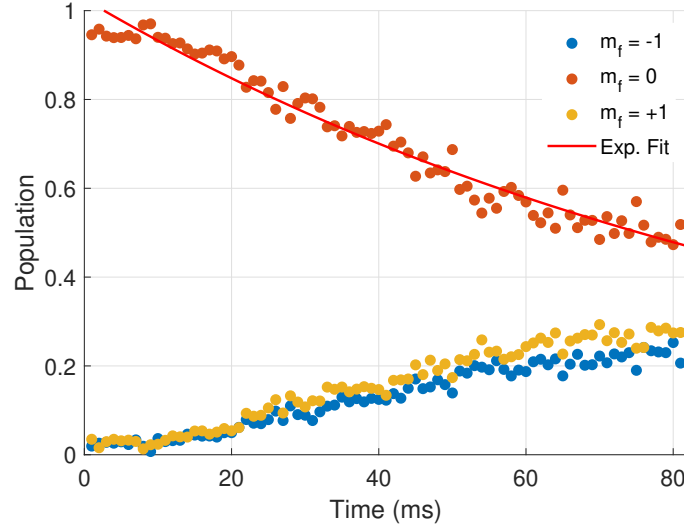


Figure 2: Inelastic collisions - We measured the population in different spin states m_f of total spin $F = 2$. The population in $|2, 0\rangle$ decays, while the population of $|2, -1\rangle$ and $|2, 1\rangle$ increases almost by the same amount as a result of inelastic collisions of atoms in state $|2, 0\rangle$, transferring them to states $|2, -1\rangle$ and $|2, 1\rangle$. From an exponential fit we estimate the spin relaxation time to be 105 ± 2 ms. It does not have an effect on the phase shift in our measurement for the magnetic insensitive transition, and only causes a slightly decreased coherence of our fringes.